

# Effects of sparger geometry on the mechanism of flow pattern transition in a bubble column

M. Vijayan, H.I. Schlaberg, M. Wang\*

*School of Process, Environmental and Materials Engineering, University of Leeds, Leeds LS2 9JT, UK*

## Abstract

Electrical resistance tomography (ERT) is used to measure void fraction wave characteristics and to identify flow pattern in a bubble column reactor (0.24 m diameter, 2.75 m height). The effects of column pressure and superficial gas velocities for different sparger geometry and for different flow pattern have been investigated. The ERT sensor can distinguish the void fraction disturbances in different flow regimes with a good clarity. The holdup derived from ERT is in good agreement with the hold-up values measured by pressure transmitters. Different flow regimes have been identified based on void fraction properties and wall pressure fluctuations. The spectral analysis of ERT measurements yields quantitative information, such as a characteristic time and a characteristic frequency of void fraction waves, which are closely related to flow structure in the prevailing regime. The experimental observations are compared with the literature.

© 2006 Elsevier B.V. All rights reserved.

*Keywords:* Sparger geometry; Transition; Bubble column

## 1. Introduction

Gas–liquid bubble columns are widely used in chemical and bio-technological industries to carry out slow reactions such as oxidation, chlorination, alkylation and many other chemical processes. They offer many advantages over other multiphase reactors—simple to construct, no mechanically moving parts and good heat and mass transfer properties.

However, bubble column design and scale-up are still difficult tasks due to the influence of its operating conditions; reactor geometry and physico-chemical properties of each phase of reactor geometry on reactor performance are not fully understood. The influence of gas sparger on the reactor performance remains difficult to quantify and the origin of regime transitions is not yet completely understood. Hydrodynamics of gas phase has a strong influence on mixing, heat and mass transfer properties. Only recent techniques such as ERT [1,2] CARPT [3], PIV [4] and the improvements of older techniques such as LDA [5] have studied the flow behaviour of bubble column including flow pattern. But none of them have studied the propagation of void fraction disturbances in a bubble column. Only the work of Fransolet et al. [2] using ERT has shown main features of

three regimes called homogeneous, transition, heterogeneous regimes. The main objective of this study is to provide better understanding of gas–liquid mixing flow properties such as void fraction disturbances (void fraction waves) and to highlight the influence of the sparger geometry and regime transitions using ERT Technique.

### 1.1. Void fraction waves and flow regimes

Void fraction waves generally occur in bubble columns. In bubble columns gas bubbles are generated using gas spargers. This gas bubble fraction is called “void fraction”. Void fraction increases with increase in the gas velocity. As the gas velocity increases bubbles density increases, at high gas velocities bubble collision and coalition occurs. Due to this chaotic behaviour, disturbance waves are generated in the bubble column. This phenomenon is called “void fraction waves”. These waves are also called as kinematic waves. Void fraction waves play an important role in identifying flow regimes in bubble column hydrodynamics. Void fraction waves can be detected by measuring fluctuation of mean void fraction of the flow pipe section. Boure and Mercadier [6] detected void fraction waves using the capacitance method. Matuszkiewicz et al. [7] has used impedance method to detect the void fraction waves. Also in the recent past Baojiang and Dachun [8] and Gong et al. [9] have measured the void fraction waves using impedance void fraction meters. All

\* Corresponding author. Tel.: +44 1133432435; fax: +44 1133432405.  
E-mail address: m.wang@leeds.ac.uk (M. Wang).

### Nomenclature

$D$	column diameter (m)
$H$	height of radial hold-up measurement location (m)
HD	dispersion height (m)
$r$	radius of sparger orifice (m)
$R$	radius of the bubble column (m)
$U_g$	superficial gas velocity (m/s)

these studies show the general characteristics of void fraction waves but none of the method is appropriate to apply to bubble column void fraction measurement. Hence this paper will primarily focus on implementing ERT method which is new and robust to measure voidage disturbances and to identify the flow regimes.

## 2. Experimental

The bubble column setup was made with transparent PVC tube with internal diameter,  $D$ , 0.24 m and 2.75 m in length. The bubble column was operated in semi batch mode (Fig. 1). The column was made of four 0.5 m and three 0.25 m sections

using flanges. This assembly allows a great flexibility in positioning of tomography sensors. The column was filled with tap water and air at a superficial velocity of up to 0.15 m/s was fed from the bottom through a multi hole gas sparger with 184 holes of 1 mm diameter (Fig. 2). A Pt100 temperature probe was installed to measure the temperature of water. Five piezo-resistive pressure transmitters (Keller 23 S) were located on the wall of the column at 2.19 m, 1.68 m, 1.18 m, 0.67 m and 0.13 m above the sparger (P1–P5) to measure the local relative pressure. Four ERT sensors, each composed of 16 stainless steel electrodes (2.4 cm × 1 cm × 0.1 cm) were embedded in four of three 0.25 m long column sections, terminated by flanges (Fig. 3) and are connected to an ERT – Data Acquisition System (ITS – DAS 2000). The measurement strategy involving repeated current injection using all possible pairs of neighbouring electrodes, leading to 104 independent measurements which are recorded in 0.1 s.

## 3. Results

### 3.1. Estimation of hold-up profiles

Holdup is one of the important parameters to predict the flow pattern in bubble column characterization. The average gas hold-up values were measured for the different geometries

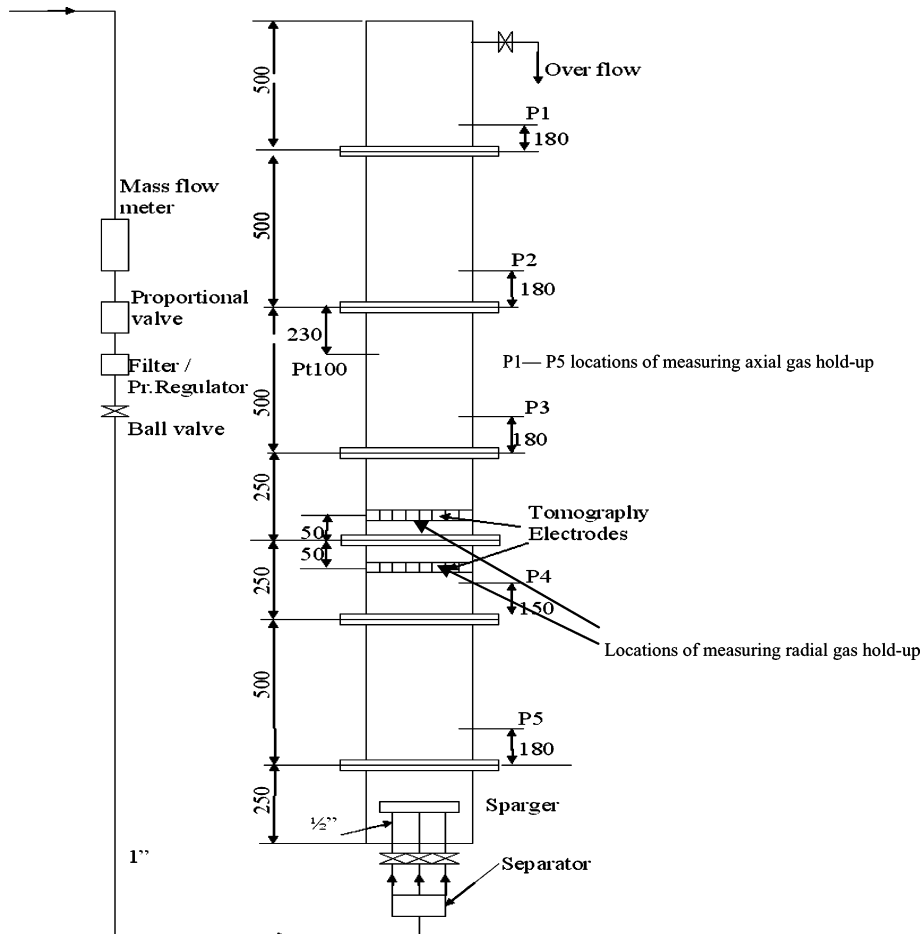


Fig. 1. Schematic diagram of bubble column with instrumentation setup.

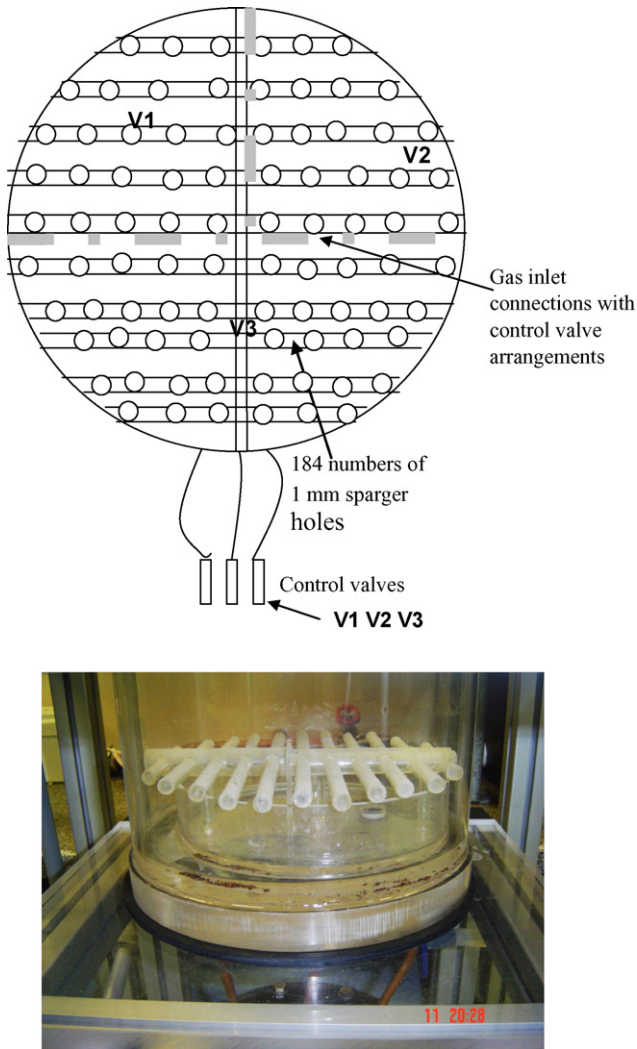


Fig. 2. Schematic diagram of enlargement view of gas distributor, 184 holes in the sparger (top); photographic picture of sparger (bottom).

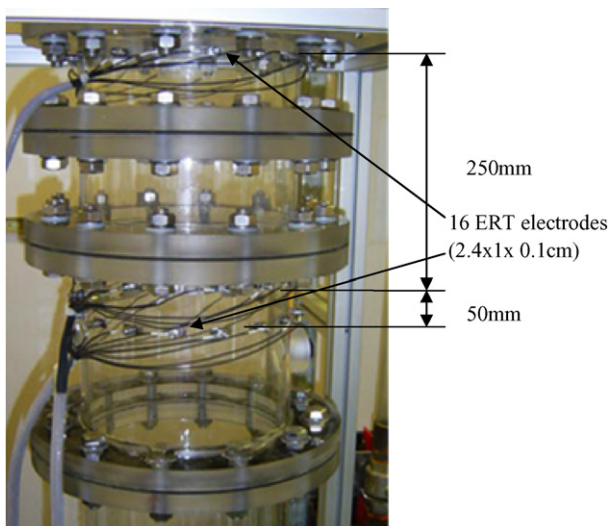


Fig. 3. ERT Electrode assembly on the bubble column.

with single quadrant, two quadrant, three quadrant and uniform sparger types. The axial gas holdup was measured at four different axial positions ( $H = 36$  cm, 88 cm, 148 cm and 200 cm) above the gas sparger using pressure transmitters. The average radial gas hold-up profiles were measured at three different axial positions (100 cm, 105 cm and 130 cm) above the gas sparger by using the 16 electrodes ERT sensor (Fig. 3). The gas holdup is defined as the summation of gas-sensor contact over the sampling time with the pressure transmitters. The local gas hold-up measurements reported in the present study are derived from ERT and pressure measurements which are less susceptible to flow disturbances.

### 3.1.1. Axial hold-up profile

The axial hold-up profile was measured for different sparger geometries over a range of gas velocities (0.01–0.15 m/s). The gas–liquid mixing (foaming) increases with the increase in the gas flow rates. This phenomenon is called dispersion height (HD). It is observed from the hold-up measurements that the height of dispersion (HD) increases with gas velocity. The maximum holdup was observed at  $HD/D = 1$ . Further increase in the gas velocity, decreases the hold-up value decreases by 15–20%. When the  $HD/D = 4–6$ , holdup decreases by 25%. A further increase in the  $HD/D$  ratio results in a marginal decrease in average hold-up value. Typical hold-up values are presented in Fig. 4(a–d). It is also observed from Fig. 4(a–d) that the holdup increases with increase in the number of sparger holes. Single quadrant sparger has low hold-up values and in the case of two and three quadrant types sparger geometries, hold-up value increases gradually. The gas bubbles generated from single quadrant sparger takes long time to become uniform when compared to the other sparger geometries. In the case of two and three quadrant spargers, time taken to obtain the uniform flow gradually decreases. In the case of uniform sparger geometry, uniform flow appears immediately and strong chaotic behaviour of void fraction waves appeared. Bubble interaction becomes stronger and bubbles coalesce rapidly. The hold-up value is distinctly high. This could be due to the disturbances during gas–liquid dispersion. Gas–liquid dispersions generate void fraction waves. As the gas velocity increases, the dispersion height is also increased. Due to this increase in the intensity of gas–liquid dispersion, high frequency void fraction waves are occurring at high gas velocity.

### 3.1.2. Radial hold-up profile

Radial hold-up profiles were measured for different sparger geometries at three axial locations as mentioned above. It is seen from the Fig. 5(a–d) that the radial holdup is increasing with gas velocity for different sparger geometries. The radial hold-up profiles are steeper at the central region of the column. In the case of uniform sparger type geometry at higher gas velocity, radial hold-up reaches the maximum value. This could be due to the occurrence of higher dispersion. Void fraction waves are formed during gas–liquid dispersion. At higher gas velocity due to higher dispersion, void fraction waves are occurring vigorously. This could lead to a localized churning flow.

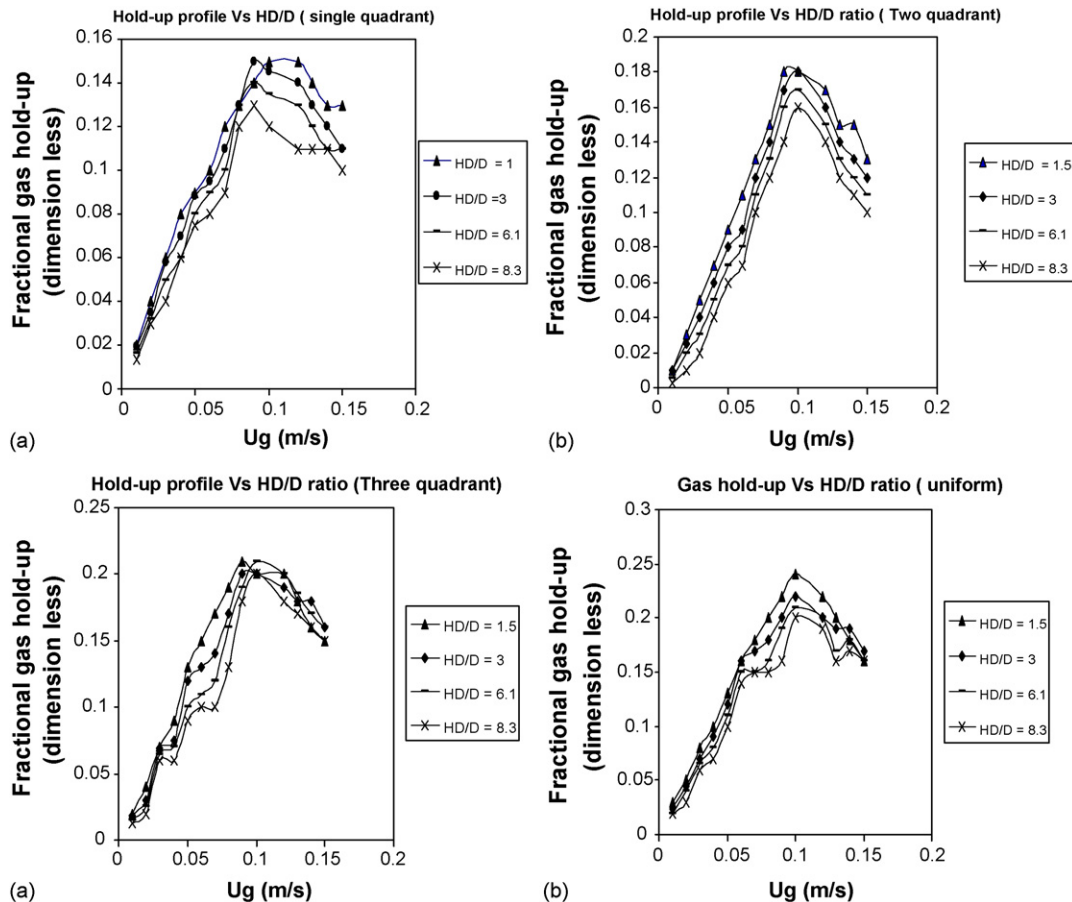


Fig. 4. (a and b) Average axial gas hold-up profiles obtained for single and two quadrant sparger geometries obtained from pressure transmitter. (c and d) Average axial gas hold-up profiles obtained for three quadrant and uniform sparger geometries obtained from pressure transmitter.

### 3.2. Comparison of axial and radial hold-up profiles with flow pattern map

Fig. 6(a and b) give the comparison of axial and radial hold-up profiles of different geometries with the literature values [2,10]. It is seen from the figure that flow regime transition occurs from bubbly flow regime to intermittent regime (Foaming regime) and further to the churn-turbulent regime at the velocities 0.07 and 0.1 m/s, respectively. Axial and radial gas hold-up profiles are in good agreement with the literature. Axial and radial hold-up values are found to be high at high gas velocity (0.1–0.15 m/s). Void fraction waves are the main cause for the increase of hold-up value. Since the pressure generating forces like drag force and shear force are behaving chaotically at the high gas velocity, the void fraction waves behave like irregular localized churn motion. Hence, the holdup is a good indicator of the flow pattern.

### 3.3. Void fraction wave mechanism using ERT measurements

Electrical resistance tomography sensor techniques are used to estimate the void fraction using the measured values of mean concentration and volume fraction. Experiments have been conducted in different sparger geometries (a) single quadrant, (b)

two quadrant (c) three quadrant and uniform type. The conditions and the manner in which each of these occur are described below. Void fraction waves are occurring in the bubble column in all ranges of gas flow rates. At lower gas flow rates, void fraction disturbances are less and as the air flow rate increases, void fraction waves occur frequently. At high gas flow rates, void fraction disturbances are occurring significantly.

Three types of flow pattern have been observed in the bubble column based on the void fraction wave patterns observed in this study: (i) discrete bubbly flow, (ii) cluster bubbly flow and (iii) churn flow patterns. These three different flow patterns throw some light on the gas–liquid interfacial behaviour in the bubble column.

#### 3.3.1. Discrete bubbly flow

The gas phase is uniformly distributed in the liquid medium as discrete bubbles. Instantaneous time measurements show the random fluctuations with small increase in the mean void fraction value. The mean void fraction plots show fewer oscillations in the void fraction values (Fig. 7a–d). The plots show the lower values during the discrete bubbly flow regime ranging from 0.05 to 0.2. Hence, it appears from above plots that the small bubbles are generated initially during the low gas flow rates. In the discrete bubbly flow regime, bubbles are tending to be uniformly

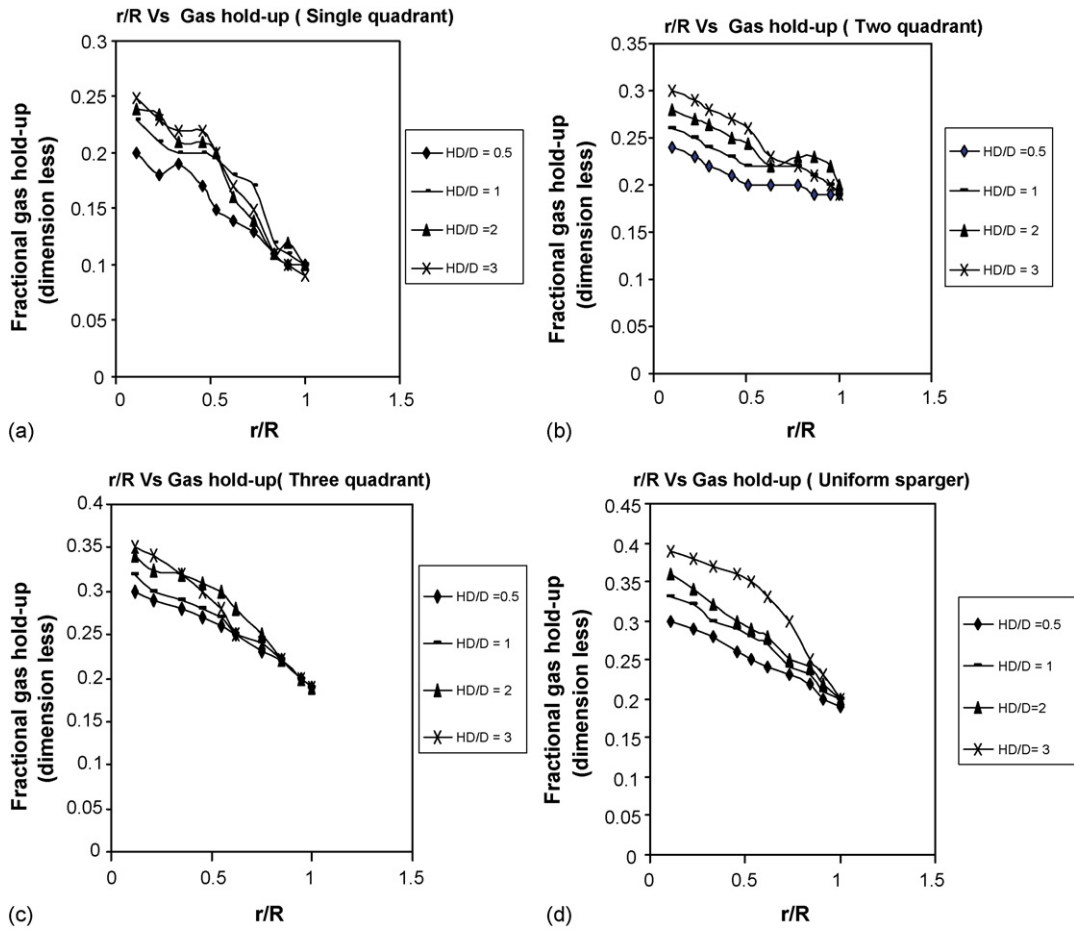


Fig. 5. (a and b) Average radial gas hold-up profiles for single and two quadrant sparger geometries obtained from ERT measurements. (c and d) Average radial gas hold-up profiles for three quadrant and uniform sparger geometries obtained from ERT measurements.

distributed. The bubble numbers density gradually increases as the gas flow is increased. The bubbles are characterized by uniform size and uniform void fraction. The bubbles generated at the sparger rise undisturbed, a small transverse axial oscillations occurs. The extent of bubble coalescence and break up is almost negligible and there is no large-scale liquid circulation in the column. A low flocculation was observed from the measurement of

bubbly regime, comparing the significant oscillation amplitude of measurement observed above 0.1.

3.3.2. Cluster bubbly flow

In the cluster bubbly flow regime, bubbles coalesce or agglomerate churn together and consequently form clusters. As they travel along the column, the bubble cluster become larger

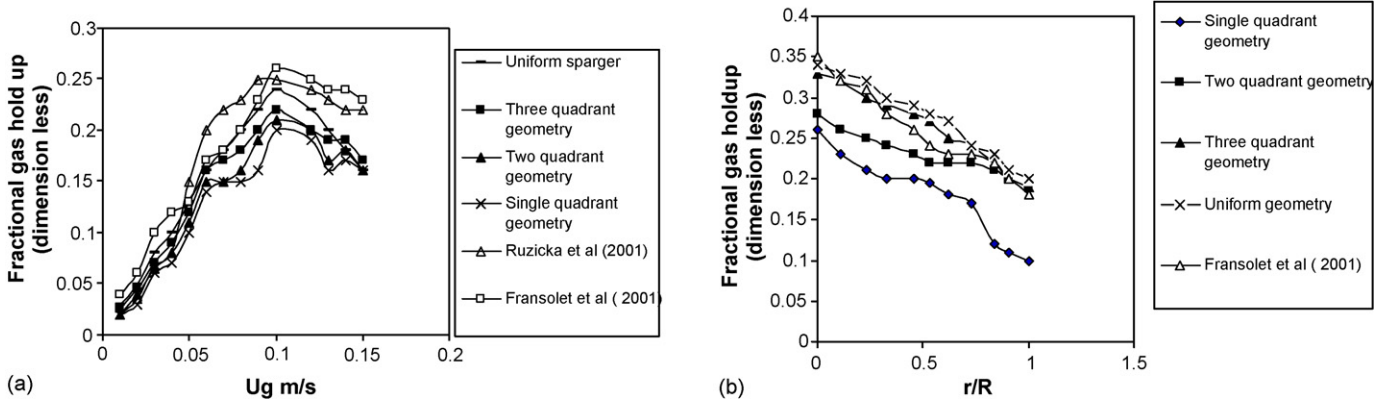


Fig. 6. (a) Comparison of axial gas hold-up profiles with literature. (b) Comparison of radial gas hold-up profiles with literature.

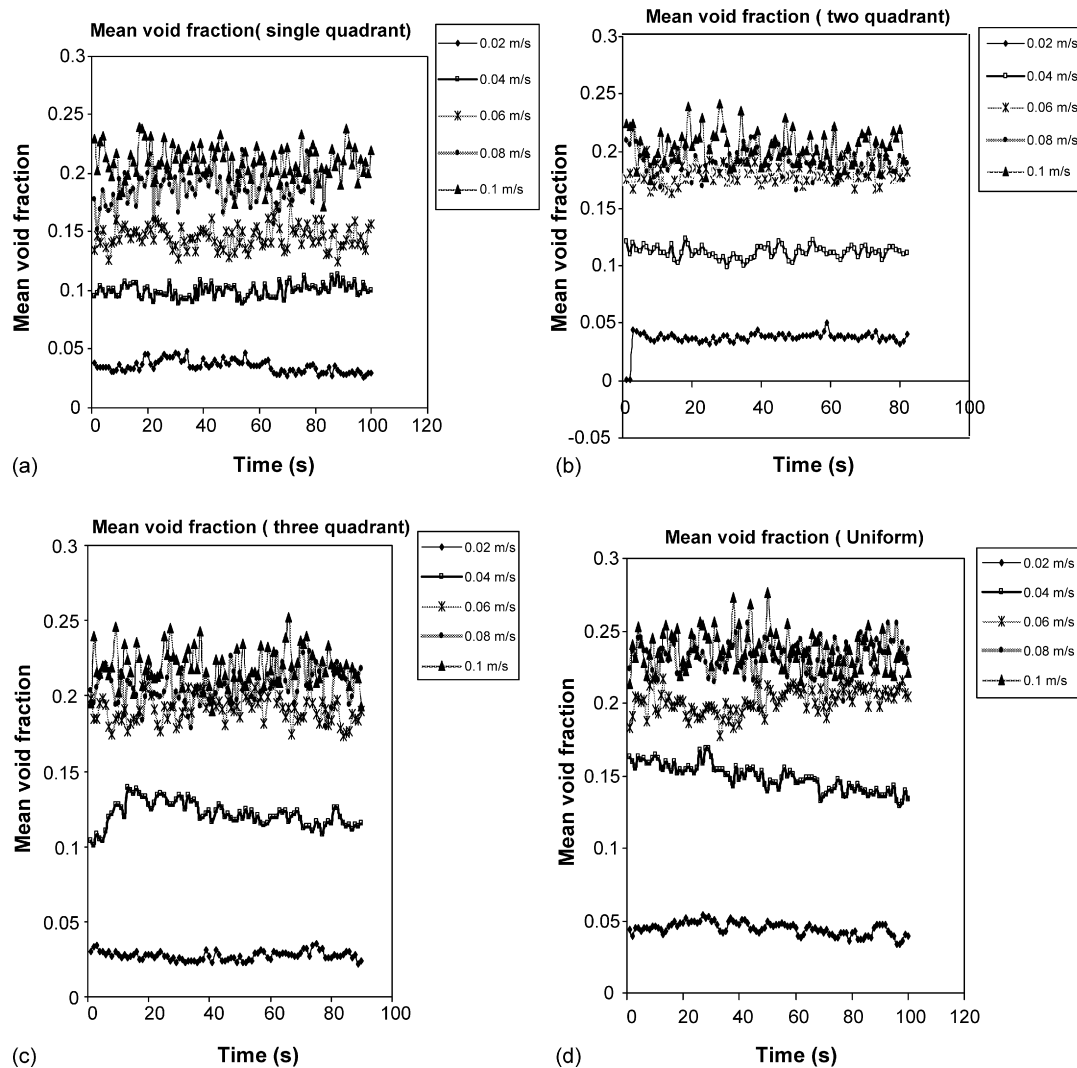


Fig. 7. (a and b) Variation of mean void fraction with air flow rate for single and two quadrant geometries. (c and d) Variation of mean void fraction with air flow rate for three quadrant and uniform geometries.

and coalesces with each other. The coalescence creates bubble fluctuations. The time record of the flow shows the apparent random fluctuation with increase in the calculated void fractions values. The mean void fraction plots show the intensity of void fraction wave disturbances gradually building up (Fig. 7a–d). The cluster bubbly flow regime is considered as transition regime between homogeneous and heterogeneous regimes. During the transition regime, the onset of bubble clustering occurs when dispersed bubble-macro eddies reaches a certain critical bubble packing state. Hydrodynamic instability occurs due to the nature of a delicate balance among uniformly dispersed bubbles.

### 3.3.3. Churn-turbulent flow

In churn-turbulent regime, abrupt coalescence of the packed bubbles appears with re-distribution of bubbles to form and distorted structure of gas phase which shows the characteristics of churn type flow. Large-scale repeated re-circulation of liquid is induced by the voidage profile with higher order of gas velocities. The unstable structures are suddenly developed with slight increase in the gas flow rate. The flow pattern observed to be very

irregular structure, which is characterised as churn flow. Localized recirculation takes place. The mean void fraction increases rapidly with increase in the gas flow rate (Fig. 7a–d). The turbulent characteristics are assumed to be isotropic and the scale of turbulence is proportional to the column diameter.

### 3.4. Effect of sparger geometry on void fraction waves

Sparger geometry influences greatly in the flow behaviour of gas liquid bubble columns. The effect of sparger has been studied by Quicker and Deckwer [11] and by Kuo [12]. In the present study, sparger was designed with 184 holes with 1mm diameter of each. The sparger has four sections of 46 holes present in each section. A separate control valve assembled for each section. Experiments have been conducted to study the influence of sparger geometry with single quadrant, two quadrant, three quadrant and uniform type sparger geometries. The ERT mean void fraction plots show the increasing trend with increase in number of sparger holes (Fig. 7). It is observed from the mean void fraction plots that the mean void fraction values are increas-

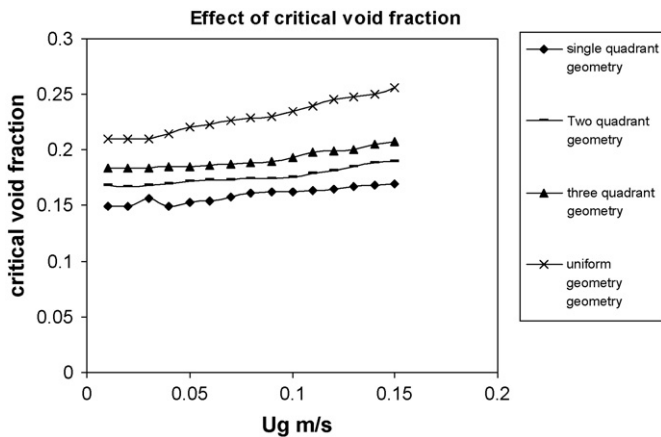


Fig. 8. Effect of critical void fraction on different sparger geometries.

ing with increase in the number of quadrants viz single quadrant, two quadrant, three quadrant and uniform type sparger geometries.

In the single quadrant sparger geometry, the mean void fraction values are increasing with gas flow rate. Typical void fraction values are obtained in the discrete bubbly regime between 0.05 and 0.2. During the cluster bubbly regime it increases up to 0.26. In the churn-turbulent regime mean void fraction values are obtained around 0.3. The mean void fraction values are less compared to other geometries (Fig. 7a). The critical void fraction values play an important role in the flow regime transition. The critical void fraction is defined as the point at which the void fraction of bubbly flow losing its stability. This critical void fraction values determine the flow regime transition. The critical void fraction plots shows that the void fraction values required for the flow regime transition is less (0.16) when compared with other sparger geometries (Fig. 8).

In the two quadrant sparger geometry, void fraction values observed are higher than the single quadrant sparger geometry which is falling between 0.05 and 0.25. This could be due to more number of bubbles generated in the column. At lower gas flow rates, the mean void fraction values oscillates less, as the flow rate is increased more oscillating trend was observed. When the mean void fraction value increases the bubble numbers also increases (Fig. 7b). The volume fraction values become unstable and deviate rapidly. The critical void fraction values are higher than the single quadrant sparger geometry (Fig. 8).

In the three quadrant sparger geometry, the mean void fraction values are higher than the single and two quadrant sparger geometries (0.1–0.26) (Fig. 7c). At lower gas flow rates, the mean void fraction values oscillates less, as the flow rate is increased more oscillating trend was observed. When the mean void fraction value increases, the bubbles become denser and larger. Localized motion increases with the increase in gas flow rate (Fig. 7c). At high gas flow rates sluggish and highly oscillating behaviour is observed. The critical mean void fraction values are higher when compared to the single and two quadrant geometries (Fig. 8).

In the uniform type geometry, the mean void fraction values are observed as the highest among all other geometries

(0.129–0.30). At lower gas flow rates, the mean void fraction values oscillate gradually; as the gas flow rate is increased vigorous oscillating trend was observed (Fig. 7d). Localized churning motion occurs vigorously. The critical void fraction values are higher than other geometries (Fig. 8).

#### 4. Conclusions

Electrical resistance tomography (ERT) measurements are used to study the effect of sparger geometry in bubble column. The data obtained from the present study show that the void fraction wave characteristics are important parameter to identify flow regimes.

Void fraction wave characteristics are found varying with different sparger geometries. Effects of column pressure and superficial gas velocities for different sparger geometry and for different flow pattern have been investigated. The ERT sensor distinguishes the void fraction disturbances in different flow regimes with a good clarity. The hold-up measured from ERT is in good agreement with the hold-up values measured by the pressure transmitters. Three different flow regimes (discrete bubbly flow, cluster bubbly flow and churn-turbulent flow) have been identified based on void fraction properties and wall pressure fluctuations. The spectral analysis of ERT measurements yields the quantitative information, such as a characteristic time and a characteristic frequency of void fraction waves, which are closely related to flow structure in the prevailing regime. Results obtained from the different sparger geometries agreeing well with literature.

#### References

- [1] M. Wang, X. Jia, M. Bennett, R.A. Williams, Flow regime identification and optimum interfacial area control of bubble columns using electrical impedance imaging, in: Proceedings of the Second World Congress on Industrial Process Tomography, Hanover, VCIPT, 2001, ISBN 0853162247, pp. 726–734.
- [2] E. Fransolet, M. Crine, G. L'Homme, D. Toye, P. Marchot, Laboratoire de Génie Chimique, B6, Université de Liège, Liège B4000, Belgium. Analysis of electrical resistance tomography measurements obtained on a bubble column, *Meas. Sci. Technol.* 12 (2001) 1055–1060.
- [3] J. Chen, S.U. Sarmobat, D.W. DePaoli, D.D. Bruns, Enhanced chaotic bubble dynamics via electrostatic fields, in: Eleventh Symposium on Separation Science & Technology, Gatlinburg, Tennessee, USA, October 17–21, 1999.
- [4] E. Delnoij, F.A. Lammers, J.A.M. Kuipers, W.P.M. van Swaaij, Dynamic simulation of dispersed gas–liquid two-phase flow using a discrete bubble model, *Chem. Eng. Sci.* 52 (9) (1997) 1429–1458.
- [5] R.F. Mudde, J.S. Groen, H.E.A. van den Akker, Application of LDA to bubbly flows, in: Proceedings of OECD/CSNI Specialist Meeting on Advanced Instrumentation and Measurement Techniques, St. Barbara, USA, 1997, p. 12.
- [6] J.A. Boure, Y. Mercadier, Existence and properties of flow structure waves in two phase bubbly flows, in: Proceeding of IUTAM Symposium, Pasadena, CA, 1980.
- [7] A. Matuszkiewicz, J.C. Flaman, J.A. Boure, The bubble-slug flow pattern transition and instabilities of void fraction waves, *Int. J. Multiphase flow* 13 (1987) 199–217.
- [8] S. Baojiang, Y. Dachun, Measurement of Void Fraction Wave in Vertical Gas–liquid Flow R.D.1998-11-17 P.D.1999-09-20, vol. 35, No. 5, 1999, pp. 646–654.

- [9] S. Gong, Yan Dachun Void Fraction waves in two phase bubble columns, *Chin. Acad. Eng.* (2004).
- [10] M.C. Ruzicka, J. Zahradnik, J. Drahos, N.H. Thomas, Homogeneous–heterogeneous regime transition in bubble columns, *Chem. Eng. Sci.* 56 (2001) 4609–4626.
- [11] K. Quicker, L. Deckwer, Bubble-size distribution in Fischer-Tropsch-derived waxes in a bubble column, *AIChE J.* 12 (1981) 123–130.
- [12] J.C.W. Kuo, Slurry Fischer-Tropsch/Mobil Two Stage Process of Converting Synthetic gas to High Octane Gasoline, Final Report DOE-PC-3022-10, DOE, 1985.